Journal of Solid State Chemistry **159,** 41–45 (2000)
doi:10.1006/jssc.2001.9125, available online at http://www.idealibrary.com on IDEAL®

AC Conductivity in the Antiferromagnetic Insulating Phase of the V_2O_3 System

H. Jhans and J. M. Honig

Department of Chemistry, Purdue University, West Lafayette, Indiana 47907

and

F. A. Chudnovskiy and V. N. Andreev

Ioffe Physical-Technical Institute, Academy of Sciences of Russia, 194021 St. Petersburg, Russia

Received January 12, 2001; accepted February 9, 2001; published online April 27, 2001

DEDICATED TO PROFESSOR BERNARD RAVEAU ON THE OCCASION OF HIS 65TH BIRTHDAY.

Measurements of the DC conductivity over more than five orders of magnitude and AC impedance over 5 Hz–13 MHz have been performed on V_2O_3 and Cr-doped V_2O_3 undergoing the antiferromagnetic insulator–paramagnetic metal phase transition. The governing factor in the explanation of the experimental results is creation of cracks during the phase transition. The electrical characteristics are interpreted in terms of the formation of metallic filaments in the insulating antiferromagnetic matrix beyond a critical frequency in applied power.

INTRODUCTION

The electrical properties of the V_2O_3 system have been extensively investigated over the past 40 years, primarily because of the variety of metal–insulator transitions that are manifest when the host is doped with Cr, Al, Ti, or excess O_2; for a review of this subject see Ref. [1]. The mechanism responsible for these transformations has been the subject of considerable debate: there is abundant evidence that electronic correlation effects are a primary driving force; however, the extensive hysteresis effects accompanying the first-order transitions indicate that the lattice also plays an important role. Among other manifestations of this effect is the extensive cracking of single crystal specimens that accompanies the first-order transition with diminishing temperature from the paramagnetic metallic (PM) state to the antiferromagnetic insulating (AFI) configuration in doped or undoped V_2O_3. As has been extensively documented elsewhere (2), such a transformation is also accompanied by a drastic change in the remnants of the magnetic order of the PM phase (that persists well above its Néel point), as compared to the prevailing magnetic order in the AFI phase. All three phenomena, electron correlations, magnetism, and lattice effects, are thus seen to be intertwined. The metal–insulator transition (MIT) in V_2O_3 inevitably leads to cracking of single crystals. Therefore, to gain a better understanding of the MIT mechanism, a closer examination of the cracking formation is needed.

In this paper we report on the effects of cracking when samples undergo the MIT, as manifested by AC conductivity measurements. The ability to investigate both the real and the imaginary components of the complex impedance provides a sensitive tool for the study of these phenomena.

EXPERIMENTAL

AC conductivity experiments were undertaken between 300 and 70 K using a standard pseudo-four-probe configuration in a commercial impedance analyzer that operated in the frequency range 5 Hz to 13 MHz. The setup was interfaced with a computer for data collection so as to obtain both the real and the imaginary components of the complex impedance $z = z' + iz''$ as a function of angular frequency ω at a series of temperatures T. Corrections were applied to eliminate contributions from parasitic elements by measuring the response to known resistive and capacitive standards in various configurations, as recommended in Ref. [3].

Pure, Cr- and Ti-doped single crystals of V_2O_3 were grown under carefully controlled conditions in a skull melter, as described elsewhere (4). The material was annealed in flowing CO/CO_2 gas mixtures at 1700 K for 8 days to achieve the desired $\frac{3}{2}$ oxygen/cation stoichiometry, and then drop-quenched. Electrical contacts to the sample were made using indium; silver paint was employed for

0022-4596/01 $35.00

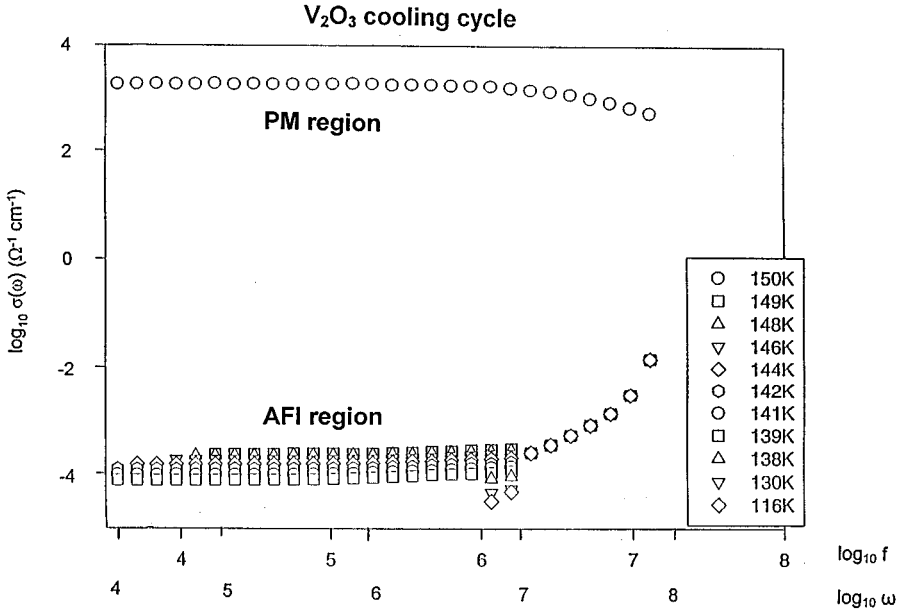

FIG. 1. $\mathrm{Log}_{10}\sigma(\omega)$ vs $\log_{10}\omega$ and $\log_{10} f$ plots above and below T_c at several temperatures—cooling cycle. Stoichiometric V_2O_3.

connections to the impedance meter leads. Utmost precautions were taken to ensure good ohmic contacts, so as to avoid erratic impedance behavior at lower temperatures. Data were collected during the first cooling and reheating cycle.

Stoichiometric V_2O_3

We display in Fig. 1 the variation of the AC conductivity $\sigma(\omega)$ with frequency f and circular frequency ω at a series of fixed temperatures while cooling stoichiometric V_2O_3; corresponding data for the heating cycle are exhibited in Fig. 2. The upper data set pertains to the properties of the PM phase. As anticipated, for the metallic domain there is little dispersion in the accessible frequency range below 13 MHz. Beyond that point one observes in Fig. 1 the onset of the dispersion effects for the metallic phase. The lower data sets pertain to properties of the AFI phase. It is seen that for frequencies f_c up to approximately $2\times10^6\,\mathrm{s}^{-1}$ and $4\times10^6\,\mathrm{s}^{-1}$ on cooling and heating ($\omega_c = 13$ and

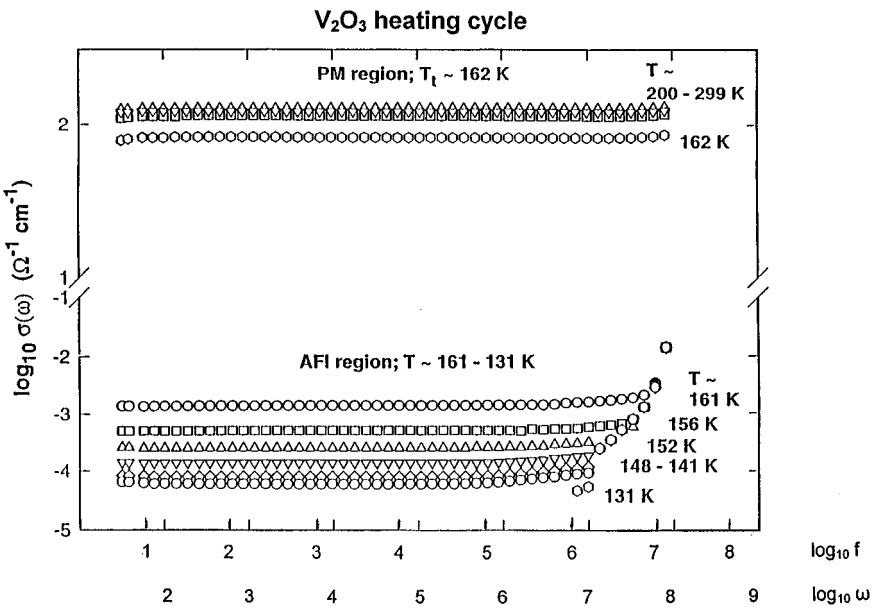

FIG. 2. $\mathrm{Log}_{10}\sigma(\omega)$ vs $\log_{10}\omega$ and $\log_{10} f$ plots above and below T_c at several temperatures—heating cycle. Stoichiometric V_2O_3.

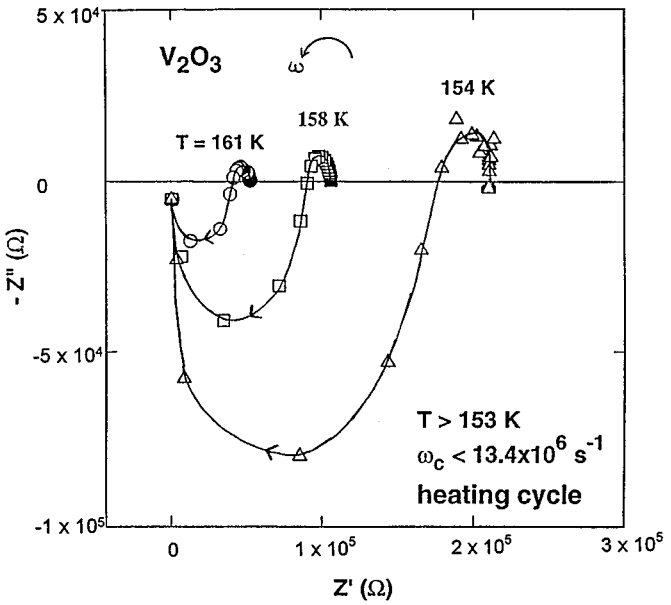

FIG. 3. $-z''$ vs z' Cole–Cole plots for V_2O_3 in the range $161 \geq T \geq 154$ K. Arrow points in the direction of increasing frequency.

$50 \times 10^6\ s^{-1}$, respectively) the dispersion is very weak; beyond this point a small discontinuity in $\sigma(\omega)$ is observed, followed by a sharp rise of σ with ω. This latter variation is rationalized in the context of the discussion of Fig. 3; the rise is approximated by the power law $\sigma = \omega^p$, where $p \geq 2$, independent of temperature.

In Fig. 3 we exhibit the AC response data in the range $154 \leq T \leq 161$ K for specimens in the AFI phase as conventional Cole–Cole plots of $-z''$ vs z'; the arrow points in the direction of rising frequency. At lower ω (higher z') the arcs fall into the first quadrant of the (z'', z') plots, while for higher ω they arcs fall in the fourth quadrant. These arcs (called ZARCs in Ref. [5]) form semicircles with their centers off the abscissa when the plots are properly scaled. The ZARCs in the first quadrant are typical of those for equivalent circuits with parallel resistive and capacitive components. The data in the fourth quadrant, however, can be mimicked only by introducing inductive components. Raistrick *et al.* (5) have briefly discussed such data in terms of pseudoinductive elements that may alternatively be considered as negative capacitances in circuits where the current leads rather than lags the applied voltage by $\pi/2$.

Cr-Doped V_2O_3

In Figs. 4 and 5 we display plots of $\log_{10}\sigma$ vs $\log_{10} f$ and $\log_{10}\omega$ obtained during cooling and warming for V_2O_3 specimens doped with 1.2 mol% Cr. The upper and lower curves again refer to samples in the PM and AFI regimes, respectively. The transition temperatures are 166 and 174 K on cooling and heating, respectively; at the transition the DC resistivity changes by roughly four orders of magnitude. In the AFI regime the AC conductivity exhibits a power dispersion law $\sigma = \omega^p$ with $p < 0.8$ for $\omega < \omega_c$, beyond which σ rises sharply with ω.

Similar results were obtained with specimens containing 3 at% Cr. The z'' vs z' plots for the doped specimens are very similar to these of pure V_2O_3 (cf. Fig. 3).

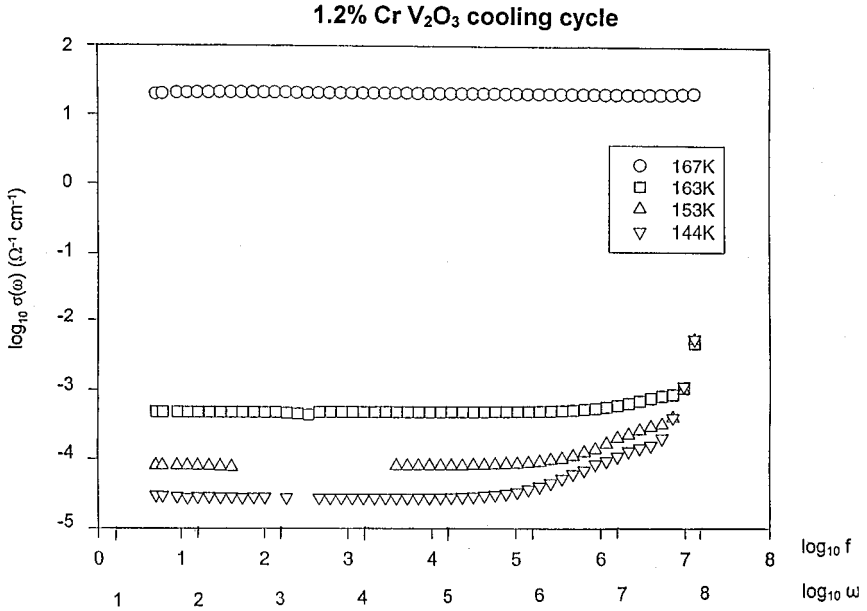

FIG. 4. $\text{Log}_{10}\sigma(\omega)$ vs $\log_{10} f$ and $\log_{10}\omega$ plots above and below T_c at several temperatures—cooling cycle. 1.2% Cr-doped V_2O_3.

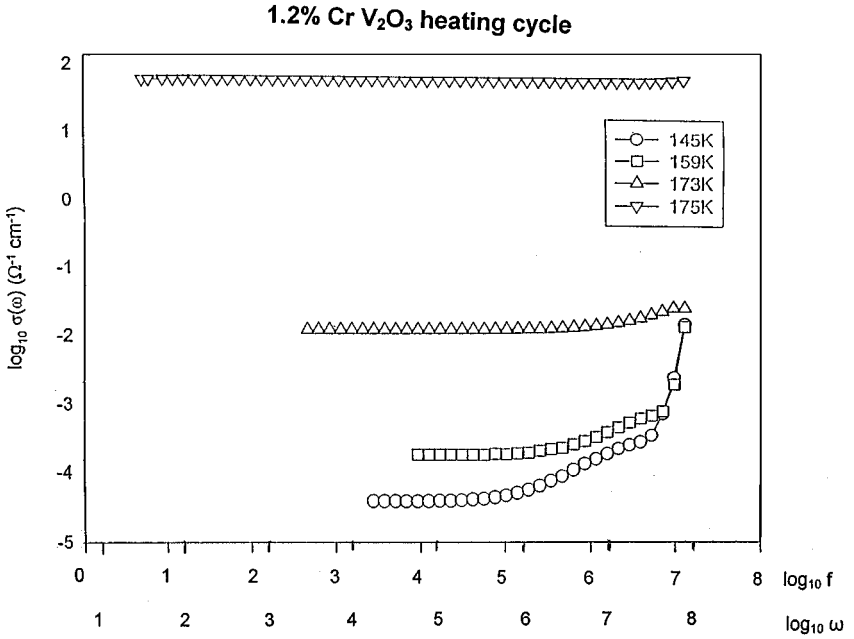

FIG. 5. $\mathrm{Log}_{10}\sigma(\omega)$ vs $\log_{10} f$ and $\log_{10}\omega$ plots above and below T_c at several temperatures—heating cycle. 1.2% Cr-doped V_2O_3.

DISCUSSION

Using acoustic emission experiments (6), carried out on crystals prepared by methods similar to those described here, cracks developed in the specimens when they were taken through the PM–AFI transition during the first cooling cycle. These cracks develop further in subsequent warming and cooling cycles across the transition. The formation of cracks on normal cooling of samples through the metal–insulator transition is also well established. Direct experimental evidence of crack formation was provided in a publication by Andreev and Chudnovskii (7), who exhibited photomicrographs of incremental crack formation on successive cycling of V_2O_3. This renders quite plausible the hypothesis that the AC conductivity anomalies reported above are due to cracking of the specimens subjected to the MIT. The following facts support this hypothesis:

1. There is a marked difference in the frequency dependence of the AC conductivity as the sample is cycled across the transition during cooling as opposed to warming.

2. The index p in the dispersion law $\sigma(\omega) \sim \omega^p$ is unusually high for frequencies $\omega > \omega_c$. As far as we know such high p values have not been reported in measurements on homogeneous media.

3. The presence of the unusual inductive component in the ZARC analysis. Our tentative explanation is as follows: Such effects have been observed (8) in VO_2 when the current and voltage exceed a critical value; current filaments then appear, rendering the sample inhomogeneous. These filaments tend to be located near sample inhomogeneities, both in the interior and on the exterior surfaces. A mechanism is provided in Ref. (8) to show how such filaments give rise to thin-film inductances. We propose that the average electric power dissipation, which rises with ω, increases up to critical value at $\omega = \omega_c$, beyond which the sample switches into an inhomogeneous state, due to generation of metallic filaments in the insulating AFI matrix. The AC conductivity for $\omega > \omega_c$ is then controlled by the nonlinear properties of the metallic filament inductances.

Nonlinearities arise because the filamentary widths as well as the real and imaginary parts of σ increase with ω. Eventually, at the highest frequencies accessible in our experiments the AC conductivity of the AFI phase approaches that of the PM phase, as documented in Figs. 1, 2, 4, and 5.

Properties of such mixed metallic and dielectric regions are usually modeled in terms of percolation theory; the behavior of the system is governed by its closeness to the percolation threshold. Let x and x_c be the fraction of the system in the metallic state and at the percolation threshold. Then the static dielectric constant $\varepsilon(x)$ of the medium near the threshold is given by

$$\varepsilon(x) = \varepsilon_o/|x - x_c|^q,$$

where q is the critical index, which, in the effective medium approximation has the value unity.

To estimate $\varepsilon(x)$ we use the relation (9) $\varepsilon(x) = 4\pi\sigma_c/\omega_c$, where σ_c is the AC conductivity at the dispersion threshold. The experimental data lead to values of ε in the range 100 to 200, which indicates that x is rather close to the critical x_c value.

CONCLUSION

The data shown here illustrate the fact that in AC conductivity experiments one must be on the lookout for cracks and other types of macroscopic defects that may develop in a set of measurements extending over a large temperature range. While AC studies are generally employed in attempts to circumvent problems that arise in the investigation of polycrystalline materials the present measurements show that extraneous features may be introduced in this process. In particular, one must be aware of nonlinearities in properties that distort the significance of the electrical characteristics being measured.

ACKNOWLEDGMENT

This research was supported on NSF Grant 96-12130 DMR.

REFERENCES

1. N. F. Mott, "Metal–Insulator Transitions." Taylor and Francis, London, 1997.
2. W. Bao, C. Broholm, G. Aeppli, S. A. Carter, P. Dai, T. F. Rosenbaum, J. M. Honig, P. A. Metcalf, and S. F. Trevino, *Phys. Rev. B* **58,** 12727 (1998).
3. R. J. Rasmussen, Ph.D. thesis, Purdue University, 1988.
4. P. A. Metcalf and J. M. Honig, *Curr. Top. Cryst. Growth Res.* **2,** 445 (1995).
5. I. D. Raistrick, J. R. Macdonald, and D. R. Franceschetti, *in* "Impedance Spectroscopy" (J. R. Macdonald Ed.), pp. 27–132. Wiley, New York, 1987.
6. F. A. Chudnovskii, V. N. Andreev, V. K. Kuksenko, V. A. Piculin, D. I. Frolov, P. A. Metcalf, and J. M. Honig, *J. Solid State Chem.* **133,** 430 (1997).
7. V. N. Andreev and F. A. Chudnovskii, *Sov. Phys. Solid State* **17,** 1966 (1976). [*Fiz. Tverd. Tela* **17,** 2957 (1975).]
8. C. N. Berglund and R. H. Walden, *IEEE Trans. Electr. Dev.* **ED-17,** 615 (1970).
9. A. L. Efros and B. I. Shklovskii, *Phys. Status Solidi* (b) **76,** 475 (1976).